BL20XU
Medical and Imaging II

1. Introduction
BL20XU, which is the only medium-length (250 m) beamline with an undulator source in SPring-8, is designed for application to various imaging techniques. A liquid-nitrogen-cooled Si double-crystal monochromator (DCM) is used to choose the X-ray energy [7.67–37.78 keV with Si(111) reflection and 12.53–61.69 keV with Si(220) reflection]. To transport a clean and coherent X-ray beam, no X-ray optical devices except the DCM and X-ray windows are installed. There are two experimental hutches: experimental hutch 1 (EH1) is located 80 m from the source, and experimental hutch 2 (EH2) is located 240 m from the source. Various types of X-ray projection imaging, such as X-ray microtomography (μ-CT), X-ray high-speed imaging, and coherent X-ray imaging, are available. By using both EH1 and EH2, two types of experiments unique to BL20XU, both of which require a long sample-to-camera distance (160 m), are possible: ultrasmall-angle X-ray scattering (USAXS) and high-energy X-ray nanotomography (nano-CT). Multiscale CT measurement combining two or more CT systems with different fields of view (FOV) and spatial resolutions is available. Two types of system are in operation. One is a combination of nano-CT and μ-CT, which enables the observation of a sample of around 1 mm diameter with a spatial resolution of 200 nm (Fig. 1) [1]. The other is based on the use of a large beam size at EH2 to realize a FOV of up to 6 mm and a spatial resolution of 1 μm. A combination of multiscale CT and X-ray diffraction CT (XRD-CT) is also available (Fig. 1). They are selected in accordance with the sample size and requirements of experiments. By using the system, the nondestructive observation of important portions (region of interest, ROI) of a sample is possible.

On the other hand, to obtain more detailed information beyond structure, such as elemental composition, an atmospheric nonexposure sample processing system was developed to extract ROIs by precisely processing samples in an atmosphere-shielded environment.

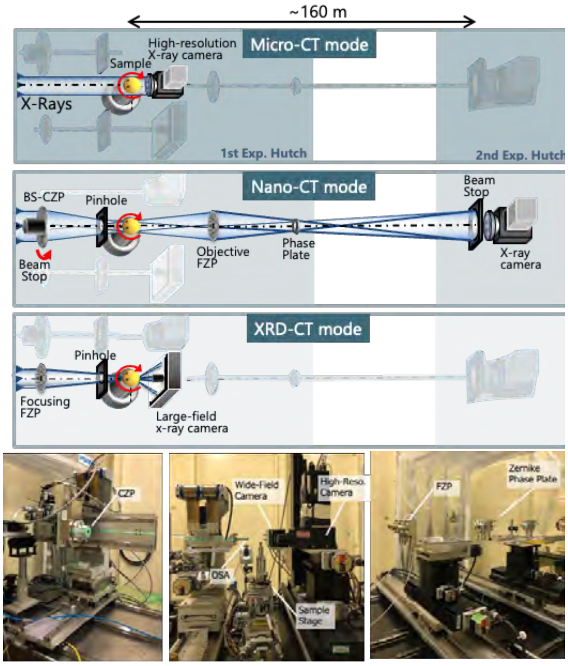

Mode	Energy	FOV	Voxel	Reso.	Scan time
Micro-CT	7.67–61.69 keV	1 mm x 1 mm	0.5 μm	1-2 μm	1 min/1800proj.
Nano-CT	15-37.78 keV	60 μm x 60 μm	25-40 nm	150-200 nm	15 min/1800proj.

Fig. 1. Schematic diagrams of multimode-multiscale CT at BL20XU consisting of nano-CT, μ-CT, and XRD (top), photograph of nano-CT setup at EH1 (middle), and typical parameters of μ-CT and nano-CT (bottom).

2. Reduction of cupping effects and ring artifacts in interior CT
The realization of noise reduction in reconstructed images under interior CT conditions has been focused on. In multiscale measurement, nano-CT measurements are inevitably conducted under interior CT conditions. In interior CT where the sample is larger than the FOV, a phenomenon called the cupping effect occurs when using conventional CT reconstruction methods such as back-projection, where pixel values, especially at the periphery of the FOV, differ significantly. Additionally, when attempting to observe fine structures inside large samples, the contrast in the image is often very weak and easily buried in background noise such as ring artifacts. This is due to the large difference in X-ray interactions between the fine structures of interest and other parts. Particularly in Fresnel zone plate (FZP) optical systems, which are diffractive optical elements, other diffraction orders become noise sources, making ring artifacts more likely to

occur, which makes image interpretation very difficult.

To remove such cupping effects and ring artifacts, two types of simple attenuation correction were introduced. Both methods are based on the idea of using an absorber/scatterer with transmittance similar to that of the sample as reference data for flat-field correction [2].

The absorption contrast CT image represents the distribution of the linear absorption coefficient of the sample μ, when the Radon transform of the absorption contrast CT is given as

$$\ln\{I(s)/I_0(s)\} = -\int \mu(x,y)dr,$$
$$r = x\cos\theta + y\sin\theta,$$

where I is the transmitted X-ray intensity of the sample, I_0 is the intensity of the reference beam without sample for the flat-field correction, and θ is the rotation angle of the CT measurement. When using the transmission image of an absorber R with uniform absorption coefficient μ_r and transmission intensity I_r as the reference data for flat-field correction, the Radon transform in this case becomes

$$\ln\{I(s)/I_r(s)\} = -\int\{\mu(x,y) - \mu_r\}\, dr.$$

Therefore, the resulting CT image shows a semi-quantitative value of the distribution of $\mu(x,y) - \mu_r$, that is, the distribution of the difference in absorption coefficients between the sample and the absorber R.

The cupping effect that occurs when the sample is larger than the FOV can be considered to occur when the values at both ends of the sinogram are nonzero. Absorption correction reduces the cupping effect when using a transmission image data of an object with a μ_r value close to the absorption coefficient of the sample as a reference beam data, bringing both ends of the sinogram close to zero. The method of applying this concept to image processing is called numerical absorption correction (NAC). NAC numerically removes the cupping effect by linear interpolation so that both edges of the sinogram become zero.

Absorption correction by absorbers is also effective in removing ring artifacts caused by errors in flat-field correction. One of the main causes of correction errors is the unevenness of the detector sensitivity. By actually using the transmission image of a uniform absorber R with absorption close to that of the sample as the reference value I_r, the difference between I_r and the intensity I of the transmission image of the sample can be reduced, suppressing errors due to sensitivity unevenness.

In addition, full-field microscope-based CT optical systems have unique ring artifacts. Under partially coherent illumination conditions, fringes occur at the periphery of the FOV; they cannot be cancelled by flat-field correction and become ring artifacts. Furthermore, in diffraction optical systems such as FZP, scattering from the sample and overlapping of diffraction beams other than the 1st order with the image appear as striped patterns called ringing as a result of background intensity modulation and interference from the sample, and of course, these cannot be cancelled by flat-field correction and become causes of ring artifacts. Therefore, even if flat-field correction is performed by moving the sample in and out of the FOV, these artifacts cannot be removed. However, if the transmission image of a reference R with the same scattering ability as the sample is used as the reference beam I_r, I_r also exhibits ringing and scattering similar to the sample image, allowing these to be effectively cancelled by flat-field correction. Therefore, to effectively remove ring artifacts, it is expected that an ideal reference would be a uniform material with the same absorption coefficient, refractive index, and shape as the sample (i.e., the sample itself with its internal structure averaged). We call this self–absorption correction (SAC). However, in practice, it is difficult to prepare such a reference, so in actual measurements, the averaged image data of the 0–180 degree transmission images of the sample measured by CT is used as a reference.

Figure 2 shows the effects of NAC and SAC in interior CT. The sample is a piece of the Murchison meteorite about 3 mm in size. The center part of spherical crystal grains, called chondrules, was observed nondestructively by nano CT [Figs. 2(b)–2(d) and 2(b')-2(d')]. All CT images were reconstructed by the convolution back-projection method. In Figs. 2(b)–2(d), images without the sample were used for reference beams for flat-field correction, and no other corrections were applied. On the other hand, Figs. 2(b')–2(d') are CT images with NAC and SAC corrections, using the average image of 0–180 degree projections of the sample for the reference beam in flat-field correction.

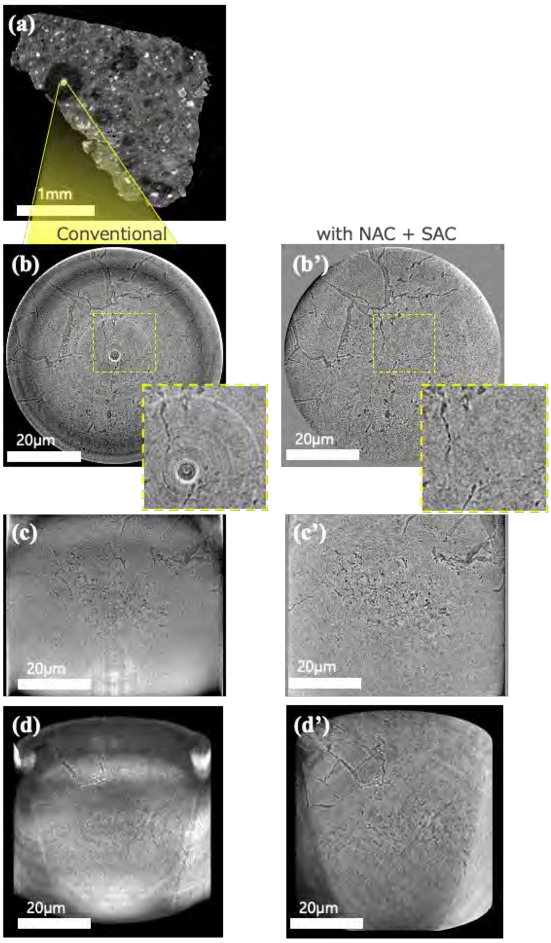

Fig. 2. Multiscale CT images of Murchison meteorite. X-ray energy is 37.7 keV: (a) μ-CT image (3 μm/voxel); (b)–(d) and (b')–(d') nano-CT images (38.9 nm/voxel). (b)–(d) Conventional reconstructed images without absorption corrections and (b')–(d') with NAC and SAC corrections. (b) and (b') CT images in the plane of rotation. Magnified view of the squared region is shown in the lower right of each image. (c) and (c') CT images in the plane perpendicular to the rotation plane. (d) and (d') 3D rendered views.

Figures 2(b) and 2(b') are CT images in the rotation plane. Comparison of the two images shows that the cupping effect is effectively removed by the two corrections. Enlarged images of the square regions in Figs. 2(b) and 2(b') are shown in the lower right of each. Sharp ring artifacts due to detector sensitivity unevenness are almost completely removed by the correction. Figures 2(c) and 2(c') are CT images of planes perpendicular to the rotation plane. The gradual artifacts seen at the periphery of the FOV in Figs. 2(b) and 2(c), which are due to ringing and scattering from the sample, are effectively removed, as seen in Figs. 2(b') and 2(d'). Figures 2(d) and 2(d') are rendering images. Without correction, because of the nonuniform field, it is difficult to render a wide range because the contrast of the fine 3D structure of the sample is overwhelmed by artifact noise [Fig. 2(d)], but with correction, all of the structures within the FOV are uniformly and clearly displayed [Fig. 2(d')].

Thus, these two corrections, although very simple and using very few computational resources, yield a robust and very powerful effect in removing cupping effects and ring artifacts. In particular, since ringing and scattering from the sample have a large impact on the signal-to-noise ratio of reconstructed images, noise removal by SAC is a very powerful tool in diffraction-type optical systems such as FZP.

On the other hand, it should be noted that SAC can only be used for interior CT and may generate new noise depending on the sample structure. Figure 3 shows interior nano-CT images of a steel sample with a diameter of 450 μm. Figures 3(a) and 3(b) are reconstructed images of the same layer, calculated without and with NAC and SAC corrections, respectively. The cupping effect, significant field nonuniformity near the center of the FOV, and fine ring artifacts seen in Fig. 3(a) are cleanly removed in Fig. 3(b), demonstrating the usefulness of the NAC and SAC corrections. On the other hand, Fig. 3(c) shows a reconstructed image of a different layer with NAC and SAC corrections. The black region with strong contrast indicated by the arrow in the figure is a void that becomes the origin of a ring artifact. The reference data must not reflect the fine structure of the sample but in cases like this sample, where there is a structure with intense contrast near the CT rotation center, taking the average of 0–180 degree transmission images may not sufficiently smooth out this structure. This can cause undesirable effects during flat-field correction, leading to ring artifacts.

As shown here, the current method of SAC correction is still not fully functional, and caution is necessary depending on the sample.

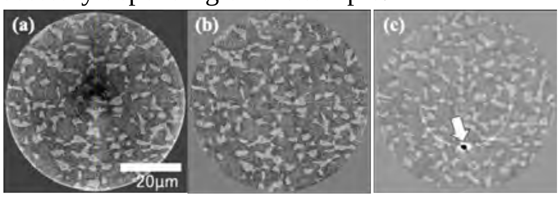

Fig. 3. Phase-contrast interior nano-CT image of a steel sample with 450 μm diameter. X-ray energy is 30 keV. (a) Reconstructed image by conventional method, (b) same layer as in (a) reconstructed with NAC

and SAC corrections, (c) another layer reconstructed with NAC and SAC corrections.

TAKEUCHI Akihisa, UESUGI Masayuki and SADA Yuki
Japan Synchrotron Radiation Research Institute (JASRI)

References:
[1] Takeuchi, A. et al. (2018). *Microsc. Microanal.* **24,** 108.
[2] Takeuchi, A. et al. (2023). *AIP Conf. Proc.* **2990**, 040012.